

## STABILITY ANALYSES AND EXPERIMENTAL INVESTIGATION OF DOUBLY CORRUGATED STEEL ARCH PANELS

Ryszard WALENTYŃSKI<sup>a</sup>, Robert CYBULSKI<sup>b</sup>

<sup>a</sup> Associate Prof.; Faculty of Civil Engineering, The Silesian University of Technology, Akademicka 5,  
44-100 Gliwice, Poland  
E-mail address: *Ryszard.Walentynski@polsl.pl*

<sup>b</sup> MSc Eng., PhD student; Faculty of Civil Engineering, The Silesian University of Technology, Akademicka 5,  
44-100 Gliwice, Poland  
E-mail address: *Robert.Cybulski@polsl.pl*

Received: 10.02.2012; Revised: 15.12.2012; Accepted: 15.12.2012

### Abstract

This paper describes briefly the stability analyses of doubly corrugated thin-walled steel panels which are used as a solution for arch buildings and roofing structures. As an example of such system the ABM MIC 120 prefabrication technology is chosen where factory on wheels makes cold-formed arch steel buildings or roofs in a very short time period as self-supporting panels. The main problem of such structures lies in the lack of proper theoretical model of the element due to its complex geometry. In order to understand the panel behavior, linear and non-linear stability analyses have been carried out with the use of ABAQUS software. The achieved results are compared with preliminary compression tests performed on steel samples. The main aim of this paper is to show how the complex geometry of such panel influences the magnitude of axial compression critical force.

### Streszczenie

Artykuł zwięźle przedstawia analizę stateczności podwójnie giętych elementów cienkościennych, które są używane jako rozwiązanie dla budynków i przekryć dachowych. Przykładem takiego rozwiązania jest technologia prefabrykacji elementów cienkościennych zwana ABM MIC 120, gdzie mobilna fabryka produkuje w bardzo krótkim czasie zimno gięte samonośne panele do konstrukcji budynków stalowych o kształcie łuku lub łukowych przekryć dachowych. Główny problem tej technologii leży w braku odpowiedniego modelu teoretycznego tych paneli ze względu na ich złożoną geometrię. Aby zrozumieć zachowanie się paneli pod działaniem obciążeniem, liniowe i nieliniowe analizy stateczności zostały przeprowadzone w programie ABAQUS. Uzyskane wyniki porównano z wynikami otrzymanymi ze wstępnych badań laboratoryjnych przeprowadzonych na ściskanych próbkach paneli. Głównym celem tego artykułu jest pokazanie w jakim stopniu złożona geometria panelu wpływa na wielkość siły krytycznej.

Keywords: **Doubly corrugated; Cold-formed; Steel; Self-supporting; Panels, Linear, Non-linear Stability.**

## 1. INTRODUCTION

Due to today's difficult economy, cheap and short time consuming solutions for buildings industry are very desirable. One of the solutions which fulfills above requirements is the ABM (Automatic Building

Machine) technology. It is a mobile factory used to fabricate and construct K-span arch steel buildings based on self-supporting panels made of MIC 120 and MIC 240 profiles. This technology comes from the USA and belongs to M.I.C. Industries Inc.[12]. Such technology was commonly used by US army to built

temporary buildings and nowadays those structures become popular solution in civilian life. In Poland there are two companies specializing in this building system. First one, Konsorcjum Hale Stalowe [9] uses MIC 120 profiles. Second one, Węglopol Sp. z o.o. [18] uses MIC 240 profiles. Also in other European countries ABM steel buildings become popular. In Czech Republic and Slovakia such prefabrication system is offered by [8] and [13] companies. The ABM technology and similar building systems are commonly used in Russia (represented by [2]) in regions where snow load has a dominant role in load cases. In Figure 1 cross-sections of MIC 120 and 240 profiles are presented. Herein only MIC 120 profile is considered.

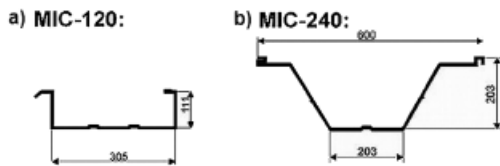


Figure 1. Cross-sections of the ABM profiles

The ABM technology consists of a movable, steel building manufacturing plant, known as the MIC 120 System. This machine is placed on a trailer, forming factory on wheels which can be easily transported to any construction sites (see Figure 2). Once, the machine is delivered to site, the construction process can be started by a small group of trained crew. Firstly, coil of steel is formed to the straight panel of channel cross-section. This panel is cut to achieve needed span of the future arch building. Secondly, this panel is bent to form the arch and its shape changes due to surfaces corrugations. Both shapes are shown in Figure 3 and it can be observed that these panels consist of main corrugation – obtained during formation of cross-section at stage 1, and secondary corrugation – folded surfaces achieved from panel bend into an arch at stage 2. This is a reason for using the term “doubly corrugated” steel arch panel. Such terminology was also used by Mang in [11].

After a few single panels are tightened together by the seam machine, they are fixed to the lifting sling and transported to the execution place by a crane (see Figure 4). These groups of panels are seamed together to form an economical and waterproof steel structure. Ready K-Span, arch steel roof made in this technology is presented in Figure 5.

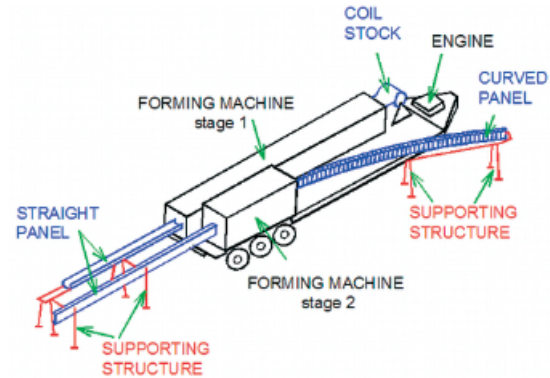


Figure 2. Prefabrication machine

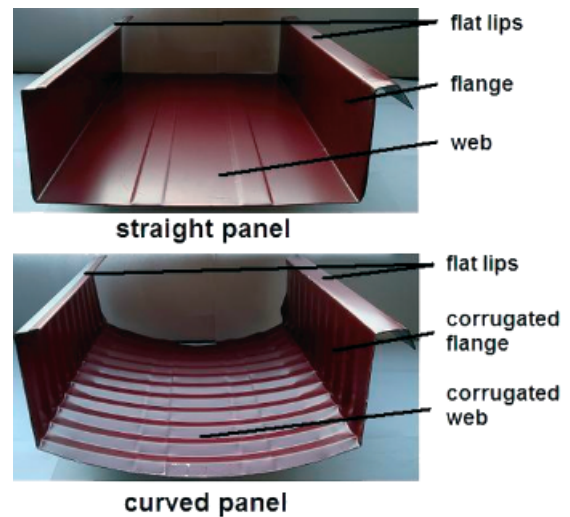


Figure 3. Straight and curved panels shapes



Figure 4. Seamed group of panels



**Figure 5.**  
ABM arch steel roof in South Korea

Precise process of construction of ABM arch steel roofs and buildings is described by US Navy Course [14] and by Walentyński in [16].

In order to understand stability behavior of straight and curved panels, linear and non-linear stability analyses in commercial FEM software ABAQUS [1] were performed. The stability behavior of ideal thin-walled element (without any imperfections) is presented by load-displacement (P-d) path diagram illustrated in Figure 6. All points at this path create so-called equilibrium path.

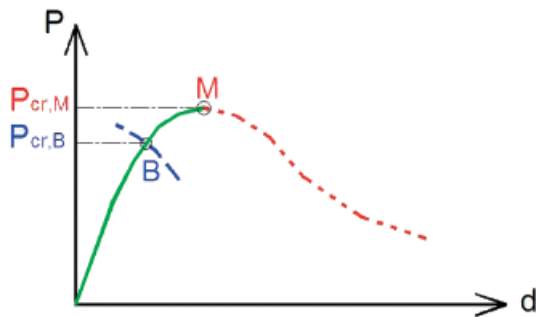


**Figure 6.**  
Load – displacement path diagram

$P_{cr,B}$  stands for critical force obtained due to bifurcation instability. In such case primary path, marked in green, which runs through the origin of co-ordinate system, intersects with secondary path marked in blue. The secondary path is formed when primary system of equations of considered problem has more than one solution corresponding to different position of equilibrium path. After point B is reached there is a possibility of post-critical force investigation.  $P_{cr,M}$  is the critical force which causes instability due to achievement of maximum load by the element. When solution approaches the limit point M, the element or structure often approaches a collapse.

The purpose of this paper is to establish which way of critical force evaluation is suitable for both panels (straight and curved). From existing literature [4], it is already known that using linear stability analysis, the instability point M cannot be determined. The linear analysis allows to evaluate the critical load caused by the bifurcation point B only if before there is no point M lying on the primary equilibrium path. ABAQUS with procedure of the type “linear perturbation, buckling” is used for linear stability analysis based on the solution of an eigenvalue problem. For non-linear stability analysis procedure of the type “Static, Riks” is performed. This type of analysis uses so-called arc length method based on load proportionality factor (LPF). Both types of analyses are widely discussed in [4].

## 2. STRAIGHT PANEL STABILITY ANALYSIS

In present section description of numerical model of the straight panel is conducted together with comparison of results from linear and non-linear stability analyses provided in ABAQUS.

### 2.1. Numerical properties

In order to exclude global instability behavior and only focus on the local one, 500 mm long element of the straight panel is considered. Cross-section and co-ordinate system situated at the gravity centre are shown in Figure 7. Walls marked in blue are 1mm thick and black walls have the thickness equal to 2mm. Boundary conditions (BC) of analyzed numerical model are presented in Figure 8.

Numerical model is built from shell elements and uses 15176 quad-dominated finite elements of type S4R (a 4 node doubly curved shell with reduced integration, has six degrees of freedom at each node—three translations and three rotations). Two plates at each end of the panel model are used for applying loads and supports. These plates in ABAQUS are modeled as so-called “rigid bodies”. Concentrated axial compression load placed at the gravity center of the considered cross-section is applied at the element end where BCs  $UX=UZ=0$  are used. Meshing of the FEM model is presented in Figure 9.

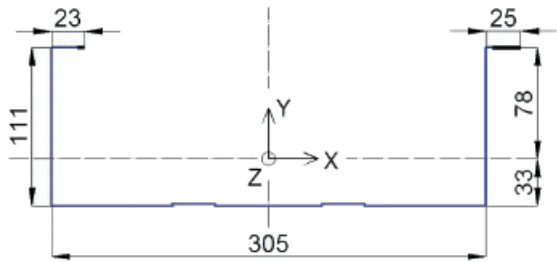


Figure 7.  
Straight panel cross-section, dimensions in mm

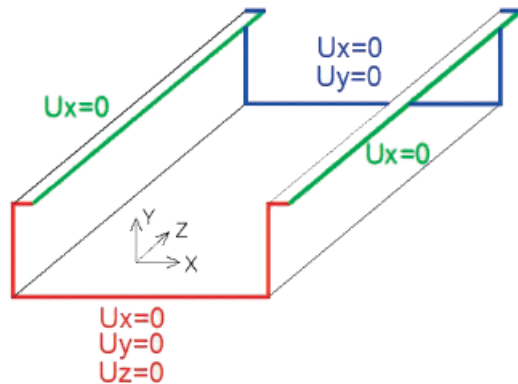


Figure 8.  
Straight panel boundary conditions

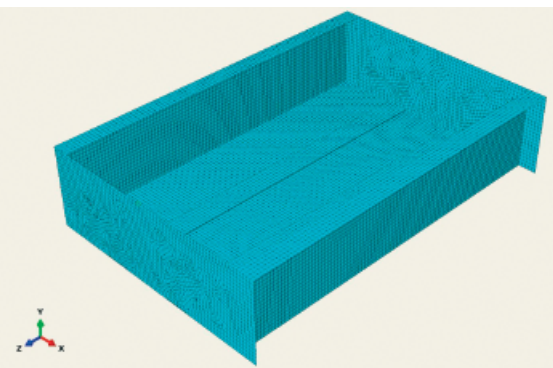


Figure 9.  
Straight panel meshing

## 2.2. Linear and non-linear stability analyses

Firstly, linear stability analysis was carried out in ABAQUS with procedure of the type “linear perturbation, buckling” based on the solution of an eigenvalue problem. Analyzed panels can be fabricated from steel grade S280GD. Young Modulus ( $E$ ) and Poisson ratio ( $\nu$ ) are equal 210 GPa and 0.3 respectively. Concentrated axial compression load in present case was chosen as 1N. First mode achieved from discussed analysis is presented in Figure 10.

From above figure it is observed that first eigen mode represents the classic plate buckling behavior where

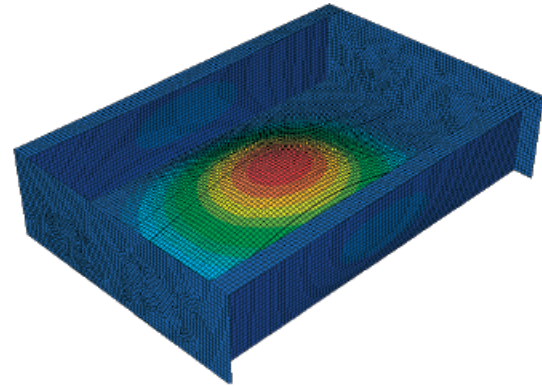


Figure 10.  
First eigen mode of straight panel (scale factor 50)

web deformations are oriented towards inside and flanges deformations towards outside. Achieved eigenvalue  $\lambda=18685$  corresponds to critical force  $P_{cr,B}$  which is equal to 18.6 kN.

Secondly, non-linear analysis was carried out in ABAQUS with procedure of the type “Static, Riks” based on so-called arc length method which uses load proportionality factor (LPF). For such analysis, basic steel plasticity model is used and for steel grade S280GD the following data is applied: Young Modulus  $E=210$  GPa, Poisson ratio  $\nu=0.3$ , yield strength  $f_y=280$  MPa, ultimate tensile strength  $f_u=424.5$  MPa and plastic strain  $\epsilon_{pl}=0.163$ . Concentrated axial compression load is equal to 18685 N and is taken from linear investigation. The deformed element due to maximum load achievement is presented in Figure 11. It is observed that deformations have also local character. Such deformation mode was achieved for  $LPF=2.68$  and this value corresponds to critical force  $P_{cr,M}$  which is equal to 50.0 kN. From non-linear stability analysis it can be concluded that obtained value of  $P_{cr,M}$  corresponds to the post-buckling critical force and deformation mode achieved for  $LPF=1$  is similar to the one shown in Figure 10. Described phenomenon is presented in Figure 12 where change of LPF during analysis is illustrated.

It is observed that LPF path changes rapidly between LPF values 0.8 and 1. Such behavior corresponds to  $P_{cr,B} = 18.6$  kN (bifurcation point B) and element instability in the form of local plate buckling occurs. It must be underlined that bifurcation point during non-linear analysis can be missed and bifurcation point was not found exactly at  $LPF=1$ . A post-buckling analysis of a geometrically perfect structure may exhibit a sharp bifurcation at the buckling load, which may be

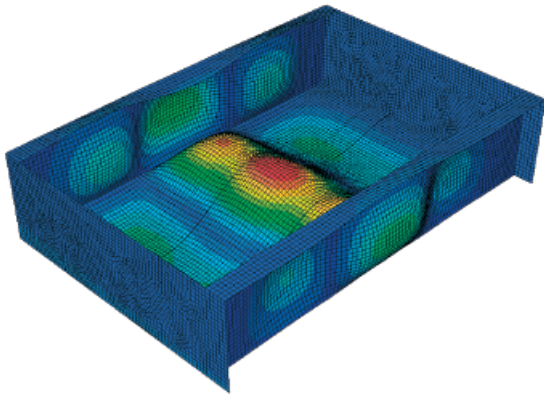


Figure 11. Deformed straight panel (scale factor 10)

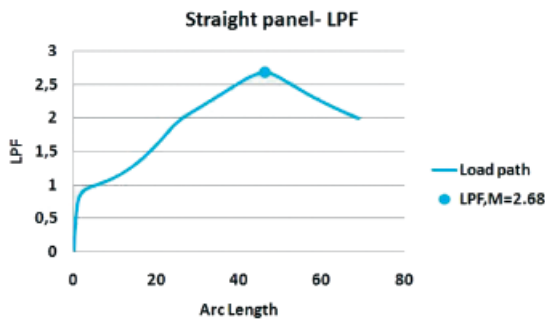


Figure 12. Load vs. analysis steps for a straight panel

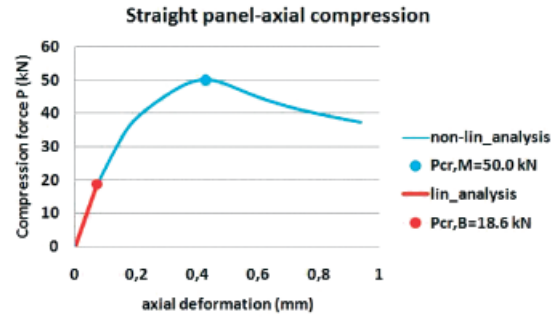


Figure 13. Load – displacement path diagram of a straight pan

missed by the Riks method. Good solution to this problem is achieved by adding geometric imperfections which smooth out the discontinuous response at the point of buckling and allows the solution to follow the response more easily. Such procedure will be used in future analyses. After LPF=1 is passed, instability points correspond to post-buckling behavior till LPF=2.68 is reached. This value of LPF is shown as a peak on considered path and corresponds to point M and to maximum load  $P_{cr,M}=50.0$  kN. At point M analyzed panel approaches a collapse.

From stability analysis of a straight panel it can be stated that bifurcation point B lies on equilibrium path before the point M which is obtained by the analyzed element due to maximum load achievement. Such phenomenon is shown in Figure 13 where relation between axial deformation (shortening of an element) and axial compression force is presented.

It can be concluded from this section, that linear stability analysis of a straight panel is applicable and estimates the critical force with big dose of safety.

Results obtained from numerical stability analyses will be compared with experimental one in the further sections.

### 3. CURVED PANEL STABILITY ANALYSIS

This section presents short discussion about linear and non-linear stability analyses of a curved panel. The simulations methodologies are similar to those presented in section 2. ABAQUS software is used for numerical analyses.

#### 3.1. Numerical properties

As in previous example, in order to exclude global instability behavior, 500 mm long element of the curved panel is considered. Cross-section, co-ordinate system and boundary conditions (BC) are presented in Figures 14 and 15. As before walls marked in blue are 1mm thick and black walls have the thickness equal 2 mm.

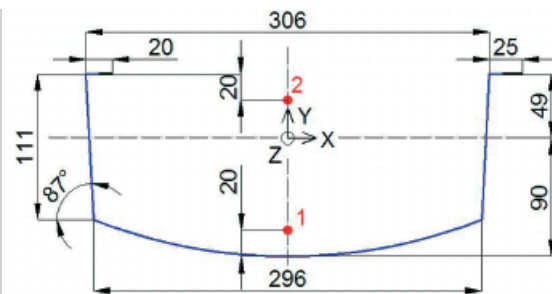


Figure 14. Curved panel cross-section, dimensions in mm

Due to complex geometry of such panels, centre of gravity was found on the empirical way by applying the concentrated compression force in different places along X an Y axes till panel shortening occurred without any cross-section vertical and horizontal displacements.

In order to build FEM model, measurement of the panel sample has been done. The sample was taken from the arch of radius 12.5 m. The dimensions of

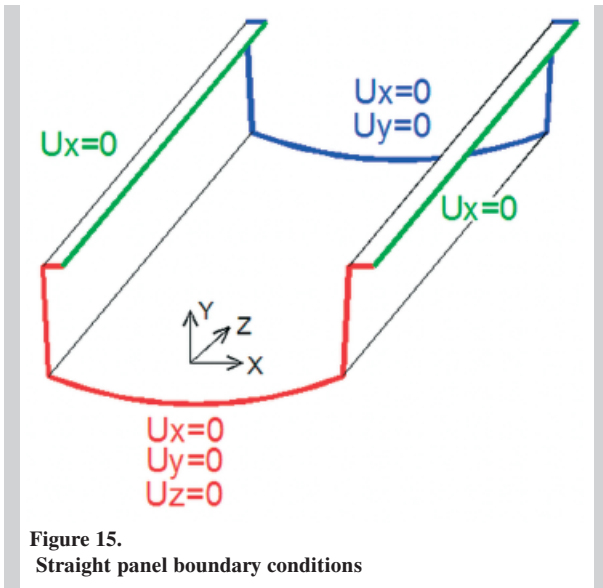


Figure 15.  
Straight panel boundary conditions

corrugations are related to span and rise of the arch. It was observed that corrugations on flanges and webs are different and it was hard to establish any pattern of their repeatability and size. After time-consuming measurements with slide caliper of many different samples, the geometry model in ABAQUS was built. The assumed geometries of surfaces corrugations are presented in Figure 16.

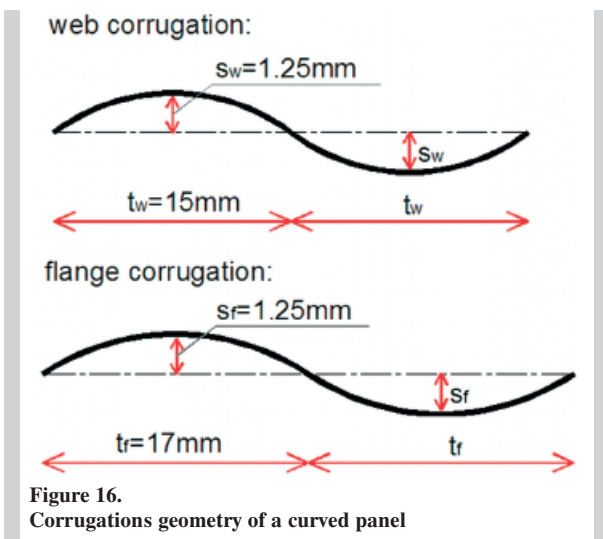


Figure 16.  
Corrugations geometry of a curved panel

Like for straight panel, numerical model was built from shell elements and uses 27244 quad-dominated finite elements of type S4R with two extra plates (“rigid bodies”) at each end for applying loads and supports. Three different load cases are considered: axial compression load applied at the gravity center

of cross-section, eccentric compression load applied at point 1 and 2 separately. Positions of these points are shown in Figure 14. FEM model meshing is presented in Figure 17.

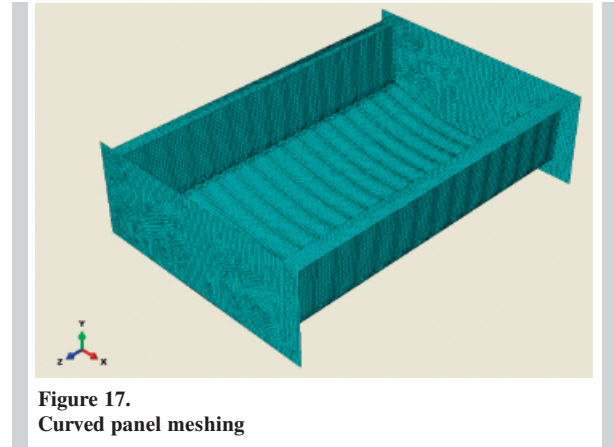


Figure 17.  
Curved panel meshing

### 3.2. Linear and non-linear stability analyses for axial compression

Firstly, linear stability analysis was carried out in ABAQUS with all necessary data given in section 2.2 of this paper.

First stability mode obtained during analysis of a curved panel has also local behavior (see Figure 18). Wider flat lip and connected to it flange deformed to waves shape. Achieved eigenvalue  $\lambda=99587$  corresponds to critical force  $P_{cr,B}$  which is equal to 99.6 kN.

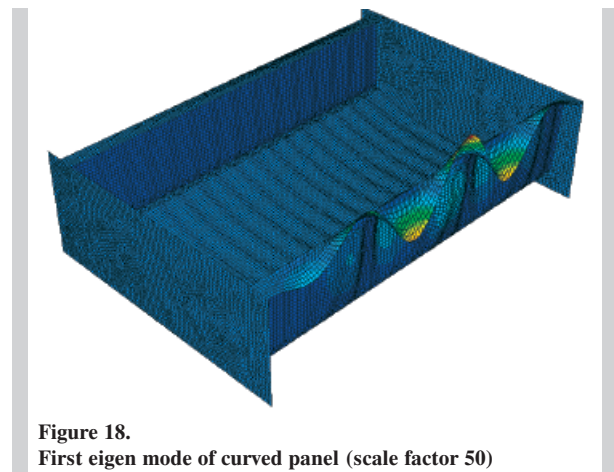


Figure 18.  
First eigen mode of curved panel (scale factor 50)

Secondly, non-linear analysis was carried out in ABAQUS with all necessary data given in section 2.2 of this paper.

Deformed element due to maximum load achievement is presented in Figure 19. It is observed that narrower flat lip from the side of applied load is destroyed and corresponding corrugations of flange and web start to squeeze.

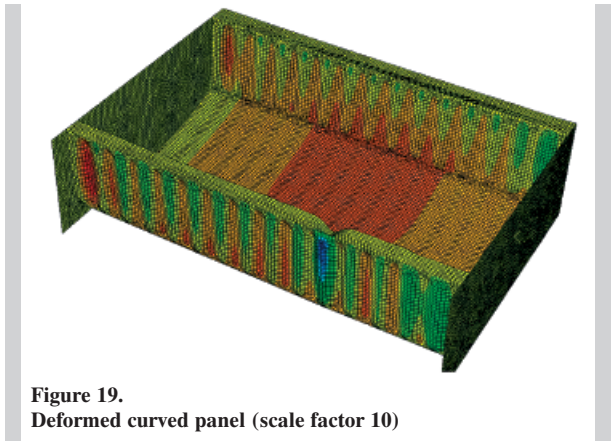


Figure 19. Deformed curved panel (scale factor 10)

Above deformation mode was achieved for LPF=0.47 and this value corresponds to critical force  $P_{cr,M}$  which is equal to 46.8 kN. The load path based on LPF values is presented in Figure 20.

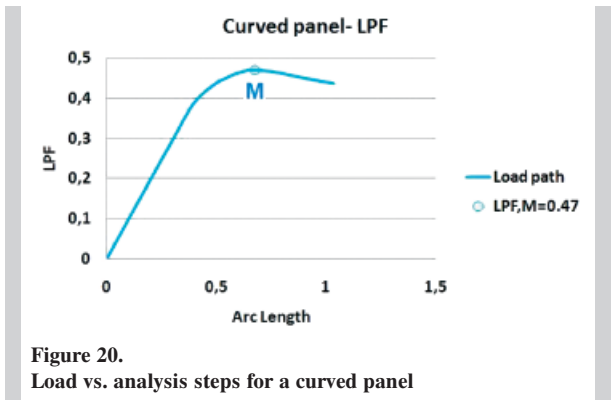


Figure 20. Load vs. analysis steps for a curved panel

It is observed the load path presented in Figure 12 and Figure 20 differ from each other. Load path based on LPF values for the straight panel has some perturbations corresponding to bifurcation instability, whereas load path course of curved panel is calm and has only one limit point M which corresponds to achievement of maximum load by the element.

From stability analysis of a curved panel it can be concluded that bifurcation point B does not lie on

equilibrium path before the point M.

Such phenomenon is shown in Figure 21 where relation between axial deformation (shortening of an element) and axial compression force is presented.

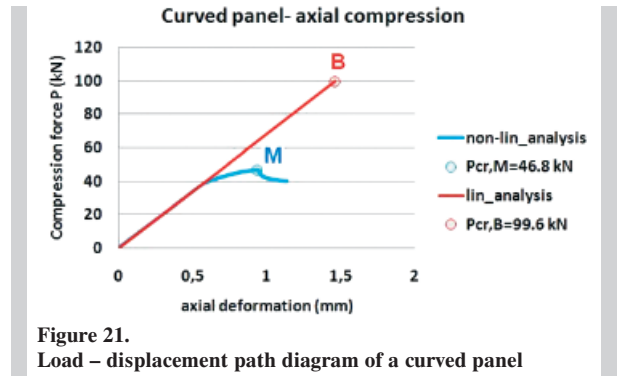


Figure 21. Load – displacement path diagram of a curved panel

It can be stated from this section, that linear stability analysis of a curved panel is not applicable due to surfaces imperfections such as corrugations and only non-linear stability analysis is able to end up with reasonable results. Introduction to numerical modeling of ABM elements is discussed by Walentyński in [17]. Results presented in this section will be compared with experimental ones in further section.

### 3.3. Linear and non-linear stability analyses for two different types of eccentric compression loads

Firstly, numerical model of curved panel with corrugated web in compression (load applied at point 1 in Figure 14) is considered. From linear stability analysis eigen value  $\lambda=119072$  which corresponds to critical force  $P_{cr,B}=119.1$  kN was found. Achieved deformation from the first eigen mode is presented in Figure 22.

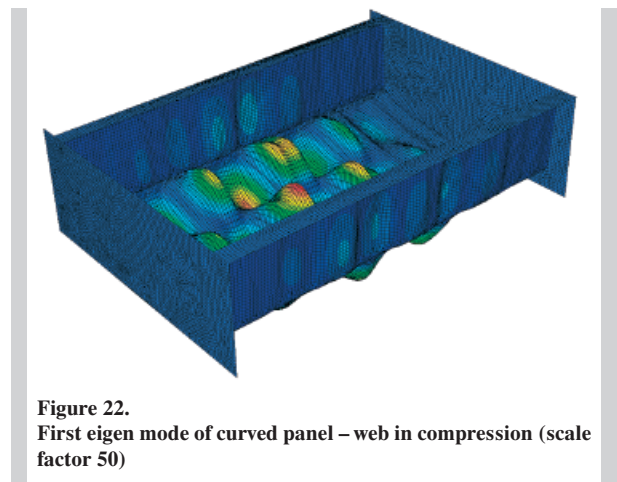


Figure 22. First eigen mode of curved panel – web in compression (scale factor 50)

Non-linear stability analysis ended up with the value of critical force equal to  $P_{cr,M}=27.9$  kN for  $LPF=0.234$ . Deformed panel due to eccentric compression is presented in Figure 23.

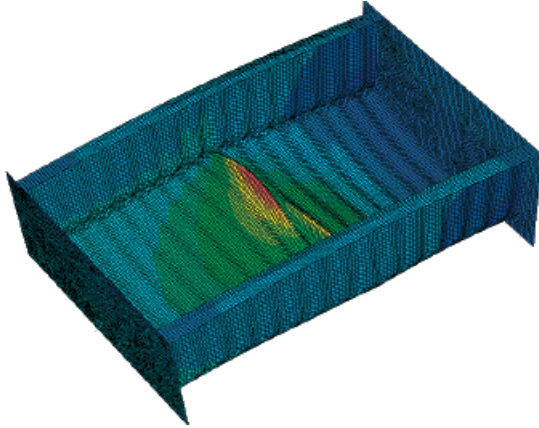


Figure 23. Deformed curved panel – web in compression (scale factor 10)

Obtained results from both stability analyses are shown in Figure 24.

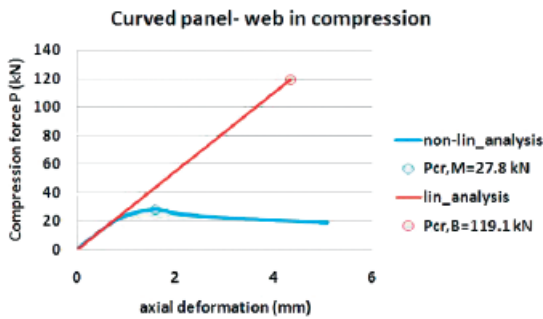


Figure 24. Load – displacement path – curved panel with web in compression

It can be also stated that linear stability analysis for present case is not applicable due to surfaces imperfections and only non-linear stability analysis gives reasonable results.

Secondly, numerical model of curved panel with flat lips in compression (load applied at point 2 in Figure 14) is considered. Achieved eigen value  $\lambda=70441$  from linear stability analysis corresponds to critical force  $P_{cr,B}=70.5$  kN. Obtained deformation from the first eigen mode is presented in Figure 25.

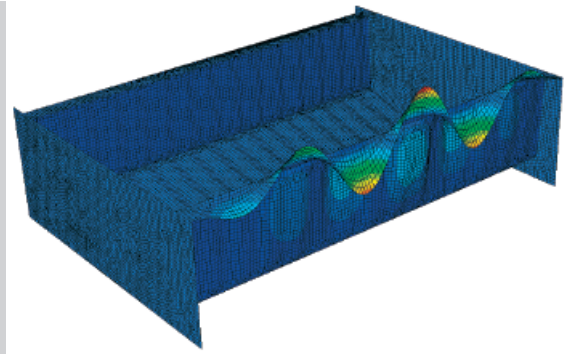


Figure 25. First eigen mode of curved panel – web in compression (scale factor 50)

From non-linear stability analysis value of critical force equal  $P_{cr,M}=33.8$  kN was achieved. Such force corresponds to  $LPF=0.48$ . Deformed panel due to eccentric compression is presented in Figure 26.

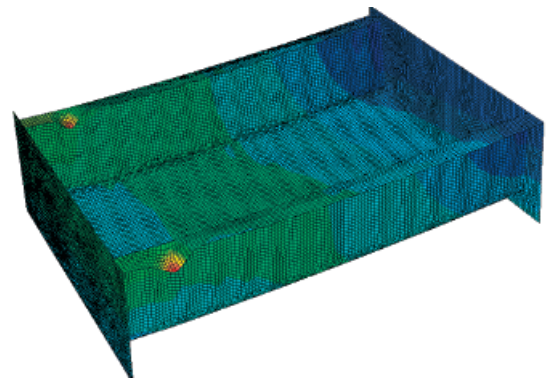


Figure 26. Deformed curved panel – web in compression (scale factor 10) pression (scale factor 50)

Obtained results from both stability analyses of curved panel with flat lips in compression are shown in Figure 27.

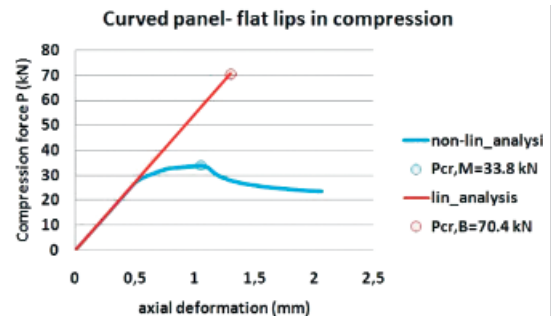


Figure 27. Load – displacement path – curved panel with web in compression (scale factor 10) pression (scale factor 50)

As before, linear stability analysis is not applicable due to surfaces imperfections. Only non-linear stability analysis is able to end up with reasonable results.

#### 4. EXPERIMENTAL INVESTIGATION

Based on experience included in articles [19] and [20] the axial compression tests of straight and curved panels (axial and eccentric compression loads) were conducted in laboratory which belongs to Civil Engineering Faculty at The Silesian University of Technology in Poland. The elements' experimental investigation at this stage of research must be called preliminary and has only qualitative meaning. Full report form described below experimental investigation is presented by Walentyński in [15].

##### 4.1. Straight panel – test set up and results

Three axial compression tests were performed on straight panels of length  $L=600$  mm. The effective length of considered samples is equal to 500 mm. Compression tests were conducted in hydraulic press. To each sample, thick metal plates were fixed due to loading transfer. On one end, this plate was 12 mm thick and on the other 2x12 mm. Cup-and-ball joint was installed between pair of plates (2x12 mm) and hydraulic press. Cross-bars were screwed down to samples in order to improve their local stabilities properties. Loading was performed in steps 0kN-5kN-0kN-10kN-0kN-15kN till samples failure. In order to measure the samples shortening, LVDT Displacement Transducer (displacement sensor no. 1) was fixed between non-movable and movable parts of hydraulic press. Such sensor was measuring the shortening of the samples. Achieved values of displacements were saddled with inaccuracies due to connections clearances between different parts of panel sample. The experimental investigations results were collected by the computer, which was connected to the test stand. Test and computer stands are presented in Figures 28 and 29 respectively.

Results obtained from experiments are presented in Figure 30 as diagrams which present relation between axial compression force (placed at the gravity centre) and axial displacement. From the curvatures shapes it can be observed that all three samples behave in the same way, furthermore it can be concluded that axial compression test was performed for each sample with similar accuracy.

Collapsed samples are presented in Figure 31. The failure mechanism of panels is similar to one

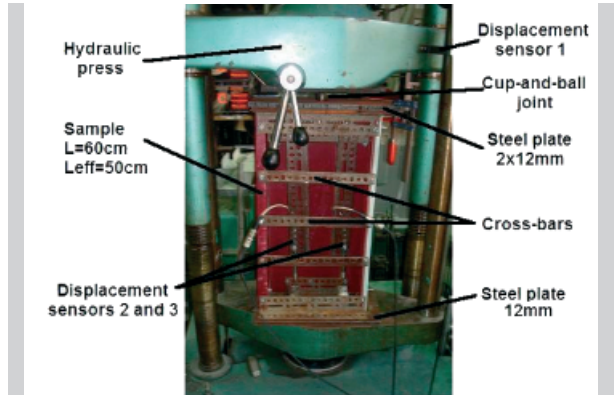


Figure 28. Test stand – straight panel



Figure 29. Computer stand

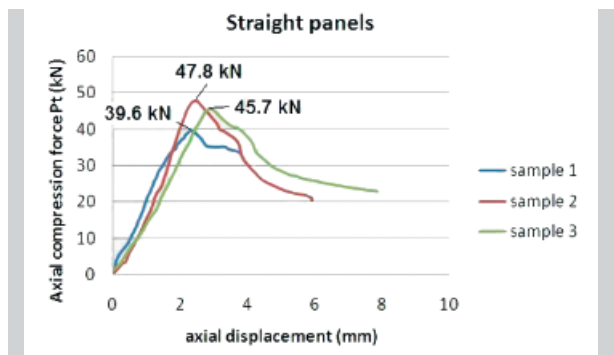


Figure 30. Experimental investigation – straight panels

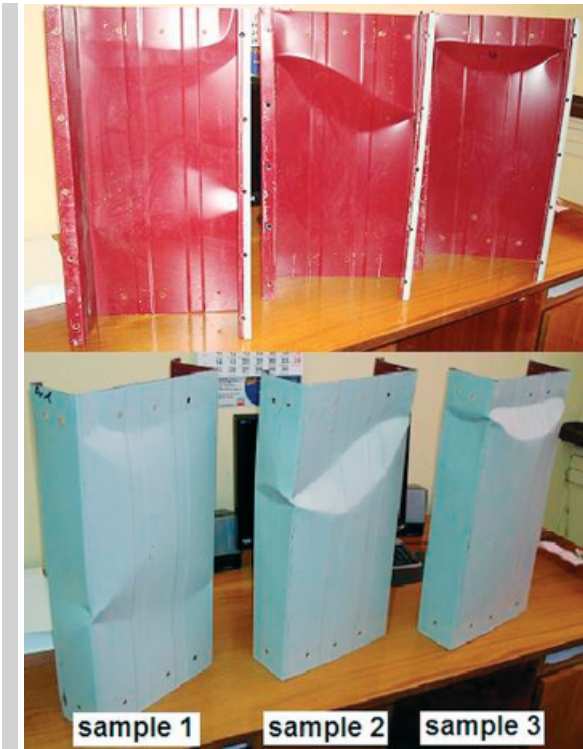


Figure 31. Collapsed samples of straight panels

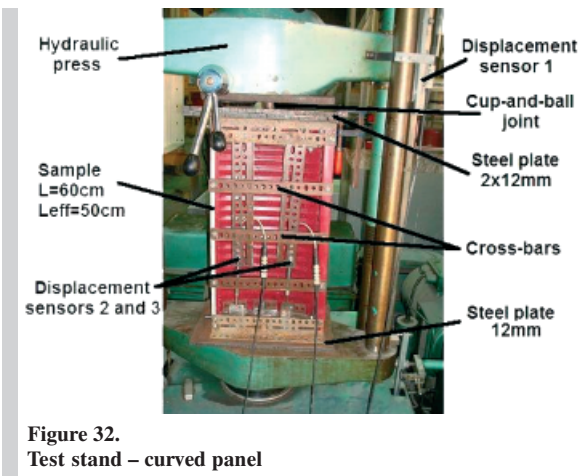


Figure 32. Test stand – curved panel

achieved from non-linear stability analysis presented in Figure 11. From these deformation shapes it can be stated that straight panel is very sensitive to the position of applied load. Even small change of such position results in change of collapse deformation shape.

#### 4.2. Curved panel – test set up and results for axial compression load

Three axial compression tests on curved panel were

conducted. Test stand is similar to the one discussed in section 4.1. As before, all three samples had displacement transducers (sensor no.1) connected between non-movable and movable parts of hydraulic press. Test stand is presented in Figure 32.

Results obtained from displacement sensor are presented in Figure 33 as diagrams which present relation between axial compression force and axial displacement (samples axial shortening). From Figure 33 it is observed that all three samples of curved panels behave in the similar way.

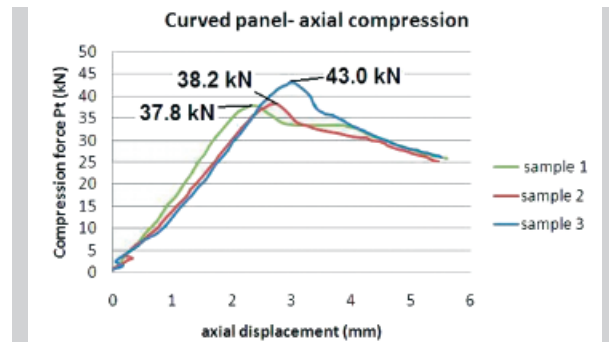


Figure 33. Experimental investigation of axial compression – curved panels

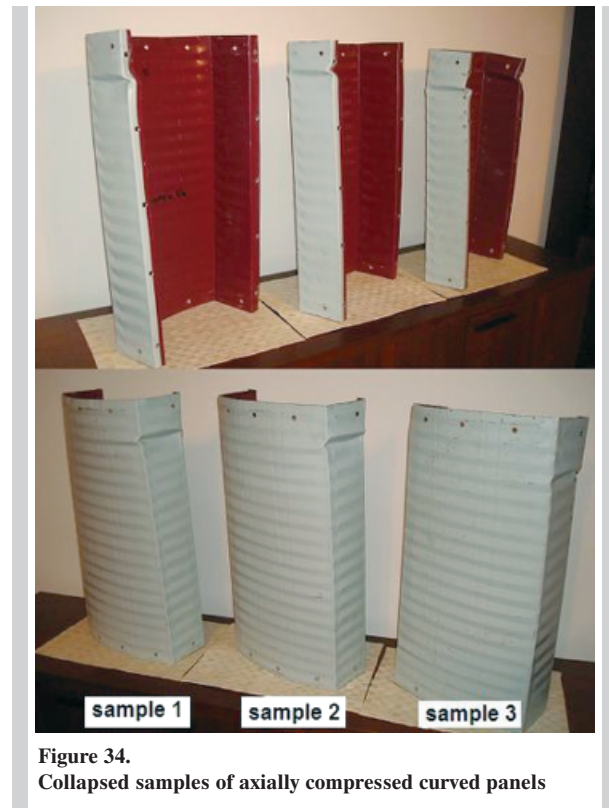


Figure 34. Collapsed samples of axially compressed curved panels

Collapsed samples deformations are presented in Figure 34. Deformed shapes of panels are similar to one achieved from non-linear stability analysis presented in Figure 19 where narrower flat lip form the side of applied load is destroyed and corresponding corrugations of flange and web start to squeeze.

From above results it can be surely stated that linear stability analysis gives inadequate results of critical forces due to complex imperfection such as surfaces corrugations.

**4.3. Curved panel – test set up and results for eccentric axial compression load**

Firstly, eccentrically loaded compression at point 1 (according to Figure 14) was applied. In present case panel’s corrugated web was in compression. Test and computer stands are similar to the ones presented in previous sections. In Figure 35 results achieved from displacement sensor are presented as diagrams which present relation between axial compression force and sample axial shortening.

Collapsed samples are presented in Figure 36. The failure mechanism of panels is similar to one

achieved from non-linear stability analysis presented in Figure 23.

Secondly, eccentric compression load at point 2 (according to Figure 14) was applied. In this case panel’s flat lips were in compression. Figures 37 and 38 present experimental results and deformed shapes of samples respectively.

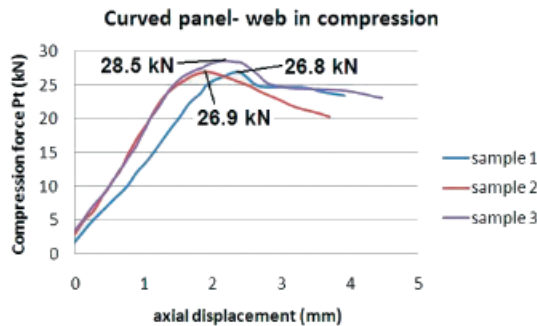


Figure 35. Experimental results – curved panels with web in compression

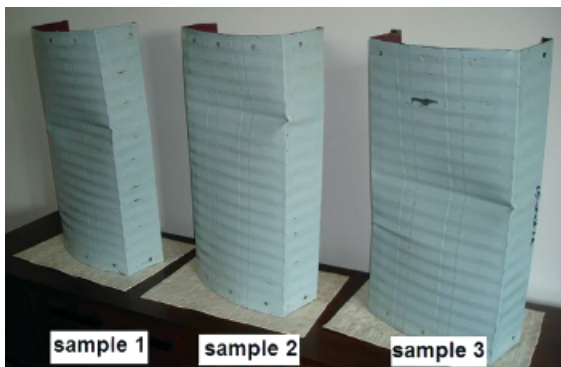


Figure 36. Eccentrically compressed curved panels at point 1

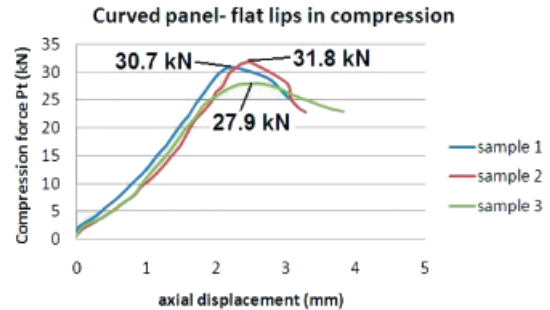


Figure 37. Experimental results – curved panels with flat lips in compression



Figure 38. Eccentrically compressed curved panels with flat lips in compression

**5. RESULT COMPARISON**

This part of the paper presents comparison of results obtained from previous sections. Firstly, comparison of results achieved from numerical analyses and experimental investigations of straight panels is provided. Secondly, results comparison between numerical analyses and experimental investigations of curved panels is presented.

In section 2.2 ( Figure 10 ) value of critical force achieved from straight panel stability analysis based on bifurcation point is presented as force  $P_{cr,B} = 18.6$  kN. Section 3.2 (Figure 18) presents critical force for curved panel which is equal to 99.6 kN.

From these two values it can be stated that corrugated walls of curved panel are less vulnerable to local buckling than walls of straight panels. For curved panels, the weakest elements from the stability point of view are the flat lips. They will always buckle before the corrugated walls.

Figure 13 presents equilibrium path achieved from non-linear stability analysis of a straight panel. It is observed that local buckling behavior at the bifurcation point occurred together with the critical force  $P_{cr,B}$  equal to 18.6 kN. After this point, the post-buckling phenomenon was studied. The post-critical force  $P_{cr,M}$  in which element reaches a collapse is equal to 50.0 kN. Three axial compression tests were carried out on straight panels samples and following maximum compression forces  $P_t$  were obtained: 39.6 kN, 45.7 kN, 47.8 kN. Setting-up of achieved values is presented in Table 1.

**Table 1.**  
Results comparison – straight panel

	Critical force	Sample 1	Sample 2	Sample 3	Average value
Experimental investigation	$P_t$ [kN]	39.6	47.8	45.7	44.4
Non-linear stability analysis	$P_{cr,M}$ [kN]	50.0			
Ratio	$P_t / P_{cr,M}$	0.79	0.96	0.91	0.89

From above Table it can be stated that numerical and experimental results of critical forces show good agreements. Experimental and numerical values of elements shortening cannot be compared at this stage of research. Tested straight panels are saddled with inaccuracies due to connections clearances between different parts of experimental samples. Failure shapes of tested samples show that straight panel is very sensitive to the position change of applied load (load eccentricity) and even small change of such position results in change of collapse deformation shape. In order to measure the shortening of straight panel during the axial compression tests, more precise experiment must be prepared with bigger amount of displacement sensors and by adding extensometers in failure areas of straight panels.

Load- displacement path, both from linear and non-linear stability analyses of curved panels under axial compression is presented in Figure 21. It is observed that value of critical force from linear stability analy-

sis is larger than value obtained from non-linear stability analysis. Critical compression force achieved from non-linear stability analysis is equal to  $P_{cr,M} = 46.8$  kN. Experimental values of compression forces (37.8 kN, 38.2 kN, 43.0 kN) are smaller than  $P_{cr,M}$ , but much smaller than  $P_{cr,B} = 101.2$  kN. Based on above results it can be stated that linear stability analysis of a curved panel is not applicable due to surfaces imperfections such as corrugations and only non-linear stability analysis gives reasonable values of critical forces which are comparable with experimental ones.

**Table 2.**  
Results comparison- curved panel under axial compression

	Critical force	Sample 1	Sample 2	Sample 3	Average value
Experimental investigation	$P_t$ [kN]	37.8	38.2	43.7	39.9
Non-linear stability analysis	$P_{cr,M}$ [kN]	46.8			
Ratio	$P_t / P_{cr,M}$	0.81	0.82	0.93	0.85

From Table 2 it can be stated that numerical and experimental results of critical forces show good agreements but with some discrepancy, where deviation between experimental and numerical results ranges from 7% to 19%. This can be caused by imprecise numerical model which does not cover all surfaces corrugations. At this point of research, comparison of samples axial shortening cannot be provided due to measurement inaccuracies.

Results comparison of curved panels investigation under eccentrically loaded compression is presented in Tables 3 and 4.

**Table 3.**  
Results comparison – curved panel with corrugated web in compression

	Critical force	Sample 1	Sample 2	Sample 3	Average value
Experimental investigation	$P_t$ [kN]	26.8	26.9	28.5	27.4
Non-linear stability analysis	$P_{cr,M}$ [kN]	27.9			
Ratio	$P_t / P_{cr,M}$	0.96	0.96	1.02	0.98

**Table 4.**  
Results comparison – curved panel with flat lips in compression

	Critical force	Sample 1	Sample 2	Sample 3	Average value
Experimental investigation	$P_t$ [kN]	30.7	31.8	27.9	30.1
Non-linear stability analysis	$P_{cr,M}$ [kN]	33.8			
Ratio	$P_t / P_{cr,M}$	0.91	0.94	0.83	0.89

From above Table it can be stated that numerical and experimental results of critical forces show good agreements.

The variation between experimental and numerical results will be covered in the future by optical 3D scanning of the real panel which will allow to prepare very accurate numerical model with all geometrical imperfections.

## 6. CONCLUSIONS AND FUTURE WORK

This paper describes briefly prefabrication process of cold-formed panels in ABM MIC 120 technology. This system is used for construction of self-supporting arch steel roofs and buildings.

For thin-walled elements very important issue as local stability behavior must be considered. In order to study local stability problems of ABM panels, linear and non-linear stability analyses were performed in commercial FEM software called ABAQUS. Attained results were compared with results obtained from preliminary experimental investigation.

It was observed that for straight panels (with smooth walls) linear stability analysis ends up with local buckling mode due to bifurcation point. Value of critical compression force at this point lies on the elastic part of equilibrium path. Such behavior of a straight panel corresponds to the class 4 cross-section described in EC3 Part 1-1 [6] and EC3 Part 1-5 [7] where general design rules for steel structures and plated structural elements are presented.

In class 4 cross-sections local buckling will occur before attainment of yield stress in the element. Such statement is not valid for curved panels where large surfaces imperfections called corrugations are machine pressed perpendicular to the panel longitudinal axis. According to the obtained results, curved panel losses its local stability due to attainment of

maximum load. There is no sign of instability on the elastic part of equilibrium path. In such case, curved panels cannot be treated as class 4 cross-sections. It means that EC3 presents the calculations methods for thin-walled members where only longitudinal corrugations (along panel axis) are applicable. This problem was shortly discussed by Biegus [3], where author agrees that EC3 does not provide any calculation algorithm for transversally corrugated thin-walled element but together with Kowal [10] they still assign the ABM cross-section to class 4.

In order to understand full behavior of ABM panels, compression test must be repeated with bigger accuracy due to estimation of correct axial stiffness. Also, bending tests must be provided due to flexural stiffness estimation. Having values of axial and flexural stiffness the design methods for such systems can be elaborated together with approachable mathematical model for engineers. Xuwei [21] has presented mathematical model of ABM panels but it is too complex for everyday use for design engineers. So far only numerical attempts for stiffness investigation were conducted by Cybulski in [5] but the research must be expanded by good laboratory tests.

## ACKNOWLEDGEMENTS

Calculations were possible due to Computational Grant CyfronetMNiSW/IBM\_BC\_HS21/PŚląska/028/2011.

The research is financed by National Science Centre based on grant no. DEC-2011/01/N/ST8/03552. Co-author of this paper R. Cybulski is a scholar under the project “DoktoRIS – scholarship program for innovative Silesia” co-financed by European Union under the European Social Fund.

## REFERENCES

- [1] Abaqus; www.simulia.com
- [2] Arch Construction; www.archconstruction.ru
- [3] Biegus A., Kowal A.; Collapse of a barrel vault hall made from cold-formed shells- in Polish, Engineering and Construction, No. 10, 2011, p.523-526
- [4] Cook R. D.; Concepts and applications of finite elements analysis, John Wiley and Sons Inc., 2002
- [5] Cybulski R., Koziel K.; Introduction to stiffness investigation of ABM K-span arch structures, 4<sup>th</sup> International Interdisciplinary Technical Conference of Young Scientists, 2011, Chapter 2, p.206-210
- [6] Eurocode 3; Design of steel structures- Part 1-1: General rules and rules for buildings, EN 1993-1-1, 2007

- [7] Eurocode 3; Design of steel structures- Part 1-5: Plated structural elements, EN 1993-1-5, 2006
- [8] Ings spol; [www.ingspol.cz](http://www.ingspol.cz)
- [9] Konsorcjum Hale Stalowe (Industrial Steel Consortium); [www.ptech.pl](http://www.ptech.pl)
- [10] *Kowal A.*; Dachy dużej rozpiętości z blachy fałdowej w technologii ABM (Large span corrugated roofs made in ABM technology), *Building materials*, Vol.6 No.454, 2010, p.7-8 (in Polish)
- [11] *Mang A. H.*; Finite element analysis of doubly corrugated shells, *Journal of the Structural Division*, No.10, 1976, p.2033-2050
- [12] M.I.C. Industries Inc; [www.micindustries.com](http://www.micindustries.com)
- [13] TAJANA s.r.o.; [www.tajana.sk](http://www.tajana.sk)
- [14] US Nav; US Navy Corse, Steel Builder NAVEDTRA 14251, Vol.2, 1996
- [15] *Walentyński R., Cybulski R., Koziel K.*; Achilles' hell of the ABM 120 doubly corrugated profiles, 9th International Conference on New Trends in Statics and Dynamics of Buildings, Slovak University of Technology in Bratislava, 2011, p.25-28
- [16] *Walentyński R.*; Design problems of cold formed light-weight ark structures, Local seminar of IASS Polish Chapter, 2004
- [17] *Walentyński R., Cybulski R., Koziel K.*; Numerical models of ABM K-Span steel arch panels, *ACEE Architecture, Civil Engineering, Environment Journal*, Vol.4, No.4, 2011; p.105-114
- [18] Węglopol Sp. z o.o.; [www.weglopol.eu](http://www.weglopol.eu)
- [19] *Wu L., Gao X., Shi Y., Wang Y.*; Theoretical and Experimental Study on Interactive Local Buckling of Arch-shaped Corrugated Steel Roof, *Steel Structures*, No.6, 2006, p.45-54
- [20] *Xu L., Gong Y., Gou, P.*; Compressive tests of cold-formed steel curved panels, *Journal of Constructional Steel Research*, No.57, 2001, p.1249-1265
- [21] *Xuwei F.*; A simplified computation model for arch-shaped corrugated shell roof, Third International Conference on Thin-Walled Structures, 2001